Recovery Lakes, East Antarctica: Radar assessment of sub-glacial water extent

K. Langley,[1,2] J. Kohler,[1] K. Matsuoka,[1] A. Sinisalo,[3] T. Scambos,[4] T. Neumann,[5] A. Muto,[4,6] J.-G. Winther,[1] and M. Albert[7]

Received 11 November 2010; revised 10 January 2011; accepted 21 January 2011; published 1 March 2011.

[1] A fast-flowing tributary of Recovery ice stream penetrates more than 500 km into the interior of East Antarctica. Recent satellite-based studies found surface features in the onset area of this tributary that indicate a significant subglacial hydraulic system, including four large smooth basins, the typical surface expression of large subglacial lakes, as well as eleven smaller areas over which ice-sheet surface elevations rapidly changed by discharge/filling of subglacial water. Here we present the first ice-penetrating radar evidence of subglacial conditions in this area. We identified a distinct ice-water interface only over a limited area within the boundaries of the investigated large smooth basins, previously hypothesized to be water-filled lakes. The radar characteristics in some areas are similar to those of a drained lake, indicating that parts of the bed are wet, but not a typical lake. We also find evidence for discrete water bodies outside of the lake boundaries. The lines of evidence indicate that the northern most two Recovery Lakes have recently drained.
Citation: Langley, K., J. Kohler, K. Matsuoka, A. Sinisalo, T. Scambos, T. Neumann, A. Muto, J.-G. Winther, and M. Albert (2011), Recovery Lakes, East Antarctica: Radar assessment of sub-glacial water extent, *Geophys. Res. Lett.*, *38*, L05501, doi:10.1029/2010GL046094.

1. Introduction

[2] The fast-flow channel of the Recovery ice stream penetrates more than 500 km inland, draining ice from a catchment comprising 8% of the East Antarctic ice sheet [*Joughin et al.*, 2006]. In the upper reaches of the Recovery catchment are four areas characterized by an exceptionally smooth, flat ice surface, which were proposed to be the surface expression of four large subglacial lakes (Recovery Lakes) [*Bell et al.*, 2007]. *Bell et al.* [2007] also argued that the Recovery Lakes are hydraulically linked to the onset of fast flow into the Recovery ice stream, suggesting a possible leakage of the Lakes. ICESat satellite altimetry detects the movement of subglacial water downstream of Recovery Lakes but not over Recovery Lakes [*Smith et al.*, 2009]. Continental-wide ice-flow modeling predicts significant subglacial water channels in a wider area including the Recovery Lake area [*Pattyn*, 2010].

[3] The lack of field evidence prevents us from determining the nature of the subglacial hydraulic system in this region. In addition to water, the other controlling components of the hydraulic system are basal geology and topography [*Anandakrishnan et al.*, 1998]. Marine sediments, deposited prior to the growth of the ice-sheet have been inferred beneath the neighboring Slessor Glacier [*Bamber et al.*, 2006; *Rippin et al.*, 2003] and beneath the lower streaming section of the Recovery catchment [*Joughin et al.*, 2006]. *Bell et al.* [2007] showed that the Recovery lakes lies along a tectonic fault, a similar setting to subglacial Lake Vostok and a lake near the South Pole, both of which have thick subglacial sediment packages beneath the water body [*Filina et al.*, 2008; *Peters et al.*, 2008].

[4] Here we examine 530 km of ice-penetrating radar data collected during the Norwegian-US IPY traverse over and between the large Recovery Lakes A and B (referred to here as LA and LB) [*Bell et al.*, 2007] and a nearby recently drained lake, R11 (Figure 1) [*Smith et al.*, 2009]. The results are used to test the hypothesis that the smooth flat ice surfaces of LA and LB delineate the extent of water-filled subglacial lakes and, in more general, to examine the subglacial environment in this area.

2. Data and Methodology

[5] We derive basal hydraulic head, anomalous bed reflectivity, and a proxy for specularity using 3-MHz ground-based radar data (see section S1 of Text S1 of the auxiliary material for details).[1] These are the primary parameters commonly used to identify subglacial lakes [*Carter et al.*, 2007; *Siegert*, 2000].

[6] The hydraulic head h is a measure of potential water flow at the ice-sheet bed [*Oswald and Robin*, 1973]. Water will tend to drain in the direction of lower hydraulic head and stay in the regions of h minima. Where the ice overburden is fully afloat over basal water, hydrostatic equilibrium is reached so that h is maintained uniform. Such areas are considered potential lakes. h is derived as:

$$h = z_{surf} - \left[1 - \frac{\rho_{ice}}{\rho_{water}}\right] \times H \quad (1)$$

where z_{surf} is the ice sheet surface elevation, ρ_{ice} and ρ_{water} are the density of ice and water respectively and H is the ice

[1]Norwegian Polar Institute, Tromsø, Norway.
[2]Department of Physics and Technology, University of Tromsø, Tromsø, Norway.
[3]Department of Geosciences, University of Oslo, Oslo, Norway.
[4]National Snow and Ice Data Center, CIRES, University of Colorado at Boulder, Boulder, Colorado, USA.
[5]Cryospheric Science Branch, NASA Goddard Space Flight Center, Greenbelt, Maryland, USA.
[6]Now at Department of Geosciences, Pennsylvania State University, University Park, Pennsylvania, USA.
[7]Thayer School of Engineering, Dartmouth College, Hanover, New Hampshire, USA.

0094-8276/11/2010GL046094

[1]Auxiliary materials are available in the HTML. doi:10.1029/2010GL046094.

thickness. We estimate an error of ±1.4 m in our calculated values of h.

[7] The bed reflectivity is derived from the radar-measured bed returned power $[P_{bed}]_{dB}$, which can be expressed in decibel scale as [*Matsuoka*, 2011]:

$$[P_{bed}]_{dB} = [S]_{dB} - [G_{bed}]_{dB} + [R_{bed}]_{dB} - 2\langle N\rangle H \quad (2)$$

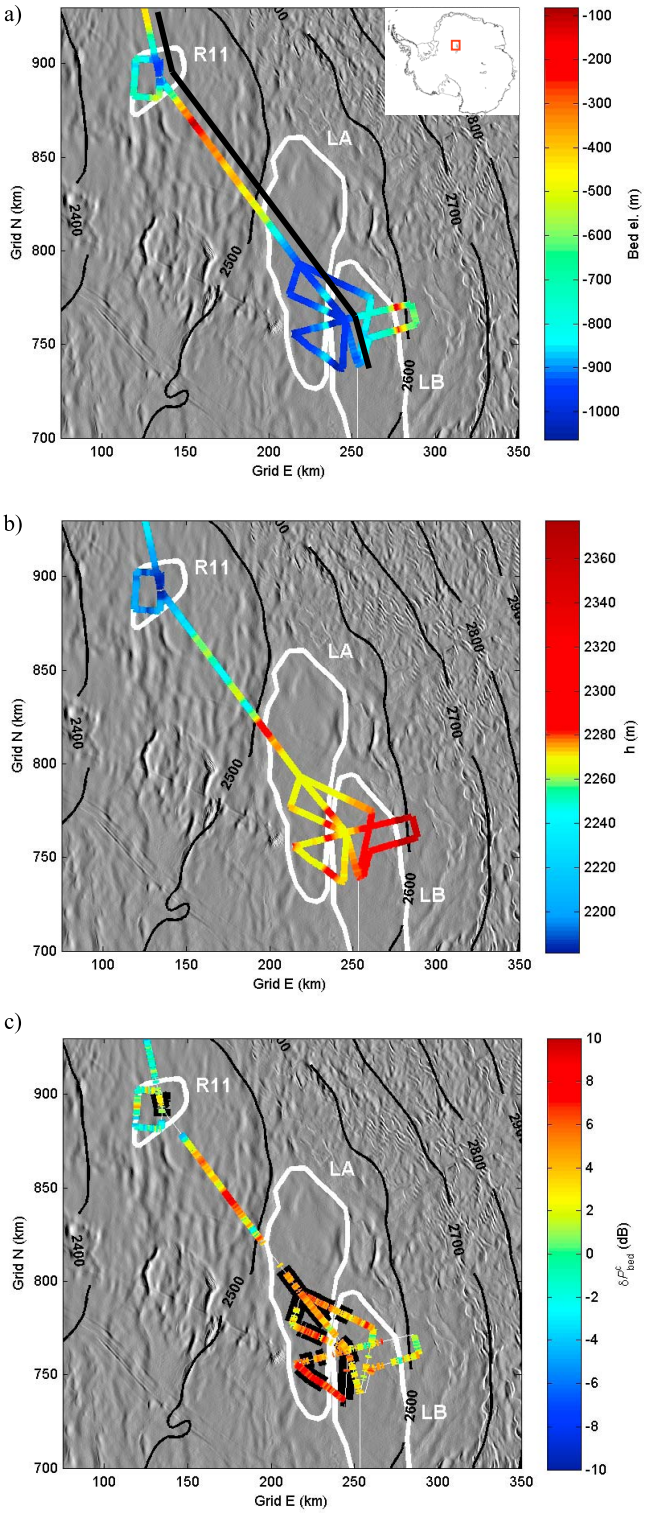

Figure 1. Radar-derived bed properties plotted with the MODIS image background [*Scambos et al.*, 2007] over subglacial lakes LA and LB [*Bell et al.*, 2007], and R11 [*Smith et al.*, 2009]. Contours show the surface elevations of the ice sheet [*Bamber et al.*, 2009] in order to show approximate directions of the ice flow. Inset shows extent of study area. (a) Ice base elevation (m a.s.l.). The location of the profile shown in Figure 2 is highlighted with the black line, offset slightly to the east of the radar track. (b) Hydraulic head, h (m). (c) A proxy of bed reflectivity $\delta[P^c_{bed}]_{dB}$. Potential lake areas, where h deviates by less than 3 m from the basin minima, are shown by the black bars.

where $[R_{bed}]_{dB}$ is the bed reflectivity, $[S]_{dB}$ is a term encompassing the radar system characteristics, $[G_{bed}]_{dB}$ is a geometric factor proportional to ice thickness H, and $\langle N\rangle$ is the depth-averaged one-way attenuation rate.

[8] We calculate the returned power $[P_{bed}]_{dB}$ in a window bounding the picked bed reflection, using half the sum-of-squared amplitudes divided by the number of samples in the window [*Gades et al.*, 2000]. $[P_{bed}]_{dB}$ is normalized by the amplitude of the direct wave, which varies up to 5 dB, to account for possible variations of instrumental factors (see section S2 of Text S1 for details). Finally, we extract $[G_{bed}]_{dB}$, approximated as the square of ice thickness, to give a corrected returned power ($[P^c_{bed}]_{dB} = [P_{bed}]_{dB} - d[S]_{dB} + [G_{bed}]_{dB} \sim [R_{bed}]_{dB} - 2\langle N\rangle H$). We reject $[P^c_{bed}]_{dB}$ with a signal-to-noise ratio smaller than 3 dB, which amounted to 16% of the entire dataset.

[9] To estimate $[R_{bed}]_{dB}$ from $[P^c_{bed}]_{dB}$, it is necessary to extract the attenuation. The depth-averaged attenuation rate can be estimated directly from the data. We linearly approximate the ice thickness dependence of $[P^c_{bed}]_{dB}$ (the relation is linear in the decibel scale, see Equation 2) and derived the ice-thickness gradient of the corrected returned power $\langle d[P^c_{bed}]_{dB}/dH\rangle$. This gradient has been widely used as a proxy of the regional-mean attenuation rate [*Matsuoka et al.*, 2010; *Matsuoka*, 2011]. From our analysis, $\langle d[P^c_{bed}]_{dB}/dH\rangle$ is −16.6. ± 3.9 dB km^{-1}, yielding $\langle N\rangle$ of 8.3 ± 2 dB/km (for one way). Data within the boundaries of the proposed lakes were not included in this analysis since this area in general has thicker ice and is expected to have a larger bed reflectivity, which may result in depth dependence of the bed reflectivity and jeopardizes the precise estimate of the attenuation rate (Equation 2).

[10] The quality of $\langle d[P^c_{bed}]_{dB}/dH\rangle$ as a proxy of regionally-averaged $\langle N\rangle$ depends on how the attenuation rate varies in this area. We estimated variations of $\langle N\rangle$ using a one-dimensional attenuation model [*Matsuoka*, 2011] for measured ice thickness data, surface temperatures [*Muto*, 2010] and recent accumulation rates from cores and shallow radar layers obtained on the same traverse. Results show that the attenuation rate is approximately constant at 8–9 dB km^{-1} for a geothermal flux in the range 50–60 mW m^{-2} (see section S3 of Text S1 for details). Therefore, in this study, we used the derived $\langle d[P^c_{bed}]_{dB}/dH\rangle$ as a proxy of the attenuation rate.

[11] Deviations of measured $[P^c_{bed}]_{dB}$ from the value predicted for an attenuation rate, estimated above, has been widely used as a proxy of bed reflectivity $[R_{bed}]_{dB}$ [*Jacobel et al.*, 2009; *Winebrenner et al.*, 2003] and is given by;

$$\delta[P^c_{bed}]_{dB} = [P^c_{bed}]_{dB} + \left\langle d[P^c_{bed}]_{dB}/dH \right\rangle H \quad (3)$$

Table 1. Summary of the Three Radar Proxies of Subglacial Lakes and Our Interpretations

Region	h	$\delta[P^c_{bed}]_{dB}$	STD	Interpretation of Basal Interface
1. South LA	Flat	High	Low	Clean ice-water interface (lake)
2. Central LA West LB	Flat	Medium	Medium	Water-rich interface
3. R11	Flat	Low	Medium	Water-rich interface, but drier than region 2 (drained lake)
Central/East LB	Gradient			
4. LA-R11 transect	Flat/gradient	High	Low	Clean ice-water interface

Thus we expect to measure higher values of $\delta[P^c_{bed}]_{dB}$ over subglacial lakes with a clean ice-water interface than over saturated sediments or surrounding grounded ice regions.

[12] The specularity of an interface has also been used to help distinguish subglacial lakes. A spatially extensive ice-water interface will give a smooth, flat, and consistently bright reflection on the radargram, compared to an ice-rock or ice-sediment interface [*Siegert*, 2000]. As a measure of specularity we use the standard deviation of $\delta[P^c_{bed}]_{dB}$ (STD) within a lateral window of 400 m, similarly to [*Carter et al.*, 2007], noting that the results are virtually unchanged for window widths of 200–1000 m. Low values of STD imply a highly specular interface, such as a clean ice-water interface.

3. Results and Discussion

[13] Now we examine basal conditions of LA, LB, R11, and the transect between these lakes on the basis of hydraulic head h, anomalous bed reflectivity $\delta[P^c_{bed}]_{dB}$, and specularity STD, together with surface features already known from satellites. Table 1 summarizes our results. The primary purpose of this analysis is to distinguish areas with a distinct ice-water interface (i.e., subglacial lake) from other interfaces with varying qualitative degrees of wetness.

[14] The distinct topographic basins of LA, LB and R11 (Figure 1a) occur at local hydraulic minima (Figure 1b), suggesting they are potential water traps. We delineated "potential lake area" within the boundaries of the lakes as areas where h deviates by less than 3 m from the basin h minima (black stripes in Figure 1c). LA contains the largest potential lake area. The east-west gradient of h in LB dictates that water will drain to the western margin of LB. At the southern part of the boundary between LA and LB is a ridge separating the two basins (Figure 1a). However, this topographic barrier and associated hydraulic isolation is not seen in the northernmost radar profile and minimum h values in LA and LB are nearly equal. This suggests that LB and LA are hydraulically connected at the north end (Figure 1b).

[15] The southernmost profile over LA is characterized by the highest $\delta[P^c_{bed}]_{dB}$ values (Figure 1c) and the lowest STD values (not shown) within the lake boundaries. Our interpretation is that the southernmost area of LA has a distinct ice-water interface and associated significant water body beneath it.

[16] The central areas of LA and western margin of LB differ from southernmost LA. h is as uniform as the southernmost LA (Figure 1b), but $\delta[P^c_{bed}]_{dB}$ is roughly 5 dB lower and STD is higher than the distinct ice-water interface of southernmost LA. This indicates that central LA and western margin of LB do not have the clear ice-water interface. Their basal interfaces are rougher and dryer than the distinct subglacial lake. The simplest interpretation of this feature is that the bed of these areas is wet, but not typical lakes.

[17] Figure 2 shows the three subglacial-lake proxies along the longest profile from south to north including LB, LA, and R11 (shown by the offset black line in Figure 1a). The central area of R11 where h is minimal (Figure 2c) has high STD values (Figure 2e) and intermediate $\delta[P^c_{bed}]_{dB}$ (red line in Figure 2d), which is lower than LA and LB but higher than the adjacent grounded ice region to the north. Therefore, we interpret the bed of R11 to be wet, although dryer than the beds of LA central and LB west. This interpretation is consistent with ICESat altimetry evidence showing that the surface of R11 lowered 20 months prior to the radar survey, suggesting that the lake drained [*Smith et al.*, 2009].

[18] Comparable radar characteristics to R11 were found in the eastern and central areas of LB (Figures 2d and 2e, 0–25 km compared to 200 km), indicating that these areas

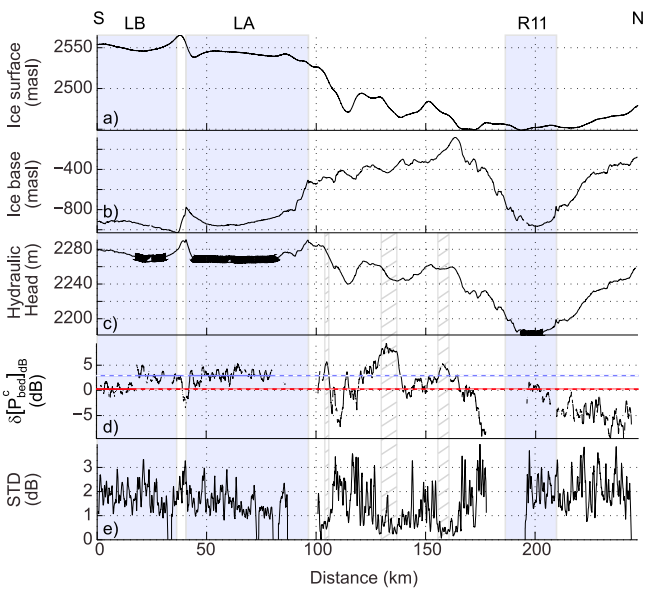

Figure 2. (a) Surface and (b) bed elevation, and (c-e) the three major radar derived proxies of subglacial lakes along the longest profile including LA, LB, and R11, shown by the black line in Figure 1a (offset to the east of the track). The grey shaded areas delimit the original proposed lake boundaries [*Bell et al.*, 2007; *Smith et al.*, 2009]. Sections crossing the uniform local h minima (+3 m) are emphasized with a thick black line in Figure 2c. In Figure 2d, red and blue solid/dashed lines show $\delta[P^c_{bed}]_{dB}$ averaged over the solid-line sections, respectively, over R11 and over western margin of LB and central area of LA. The hatched boxes indicate the intra-lake sections of large $\delta[P^c_{bed}]_{dB}$ and low STD referred to in the text.

have beds similar to R11. Because these areas have lower bed reflectivity than western LB, we argue that the bed in eastern and central LB is dryer than western LB. This is supported by the gradient in h in LB that indicates that water will drain from east to west (Figure 1b).

[19] Outside of these lake areas we find three locations where $\delta[P^c_{bed}]_{dB}$ is high and STD is low (110 km, 135 km, and 165 km), suggesting the presence of a distinct ice-water interface. Although we only have one radar line, and cannot characterize the three-dimensional potential, the area with the uniform h (extending 8 km along the profile), could be a small lake, while two sites with a significant gradient in h could be subglacial water channels oblique to the measured radar profile. Such an interpretation would be consistent with the view of an extensive and active hydraulic system in this area.

[20] Reviewing these lines of evidence, we infer that, at the time of data collection, a distinct ice-water interface, typical for subglacial lakes, exists only in southernmost LA. However, the extremely smooth surface and associated upstream troughs and downstream ridges found over LA and LB [*Bell et al.*, 2007] strongly indicate that there were significant water bodies beneath LA and LB for a significant period. Therefore, we argue that the hydraulically connected LA and LB, are most likely recently drained. Similar radar characteristics beneath the drained R11 and central and eastern LB support this interpretation. The large extent of LA and LB (8300 km^2 [*Bell et al.*, 2007]) makes it difficult to detect surface elevation changes associated with the basal drainage/inflow events. For example, the water volume (0.2 km^3) drained from R11 would lower the surface of LA and LB by only 0.025 m, which is lower than the height change criteria (0.1 m) used to identify active lakes using ICESat altimetry data [*Smith et al.*, 2009].

4. Conclusions

[21] Based on our analysis of the radar characteristics of this region (Table 1) and on the satellite evidence [*Bell et al.*, 2007; *Smith et al.*, 2009], we conclude that only the southern end of LA contains a significant water body, such that LA and LB were not water-filled at the time of the radar survey to the full extent of the boundaries inferred from their surface expression. In the rest of LA and LB, the hydraulically downstream areas have wetter conditions than the hydraulically upstream areas, where bed conditions are similar to a drained lake, R11. This new evidence leads us to conclude that LA and LB are recently drained. The volume and frequency of moving water during infilling/discharge events, and associated ice motion is of particular interest in the context of the dynamics of the onset area of Recovery ice stream and its effect on the downstream area, and ultimately on the freshwater flux from this area to the ocean.

[22] **Acknowledgments.** The authors would like to acknowledge all members of the Norwegian-US IPY traverse. This work has been carried out under the umbrella of ITASE-IDEA within the framework of IPY project number 152 funded by Norwegian Polar Institute, the Research Council of Norway and the National Science Foundation of the USA. This work is also a contribution to ITASE. We thank Robin Bell, one anonymous reviewer, and the Editor Eric Rignot for their constructive comments.

[23] The Editor thanks two anonymous reviewers.

References

Anandakrishnan, S., D. D. Blankenship, R. B. Alley, and P. L. Stoffa (1998), Influence of subglacial geology on the position of a West Antarctic ice stream from seismic observations, *Nature*, *394*(6688), 62–65, doi:10.1038/27889.

Bamber, J. L., F. Ferraccioli, I. Joughin, T. Shepherd, D. M. Rippin, M. J. Siegert, and D. G. Vaughan (2006), East Antarctic ice stream tributary underlain by major sedimentary basin, *Geology*, *34*(1), 33–36, doi:10.1130/G22160.1.

Bamber, J. L., J. L. Gomez-Dans, and J. A. Griggs (2009), Antarctic 1 km digital elevation model (DEM) from combined ERS-1 radar and ICESat laser satellite altimetry, digital media, Natl. Snow and Ice Data Cent., Boulder, Colo.

Bell, R. E., M. Studinger, C. A. Shuman, M. A. Fahnestock, and I. Joughin (2007), Large subglacial lakes in East Antarctica at the onset of fast-flowing ice streams, *Nature*, *445*(7130), 904–907, doi:10.1038/nature05554.

Carter, S. P., D. D. Blankenship, M. E. Peters, D. A. Young, J. W. Holt, and D. L. Morse (2007), Radar-based subglacial lake classification in Antarctica, *Geochem. Geophys. Geosyst.*, *8*, Q03016, doi:10.1029/2006GC001408.

Filina, I. Y., D. D. Blankenship, M. Thoma, V. V. Lukin, V. N. Masolov, and M. K. Sen (2008), New 3D bathymetry and sediment distribution in Lake Vostok: Implication for pre-glacial origin and numerical modeling of the internal processes within the lake, *Earth Planet. Sci. Lett.*, *276*, 106–114, doi:10.1016/j.epsl.2008.09.012.

Gades, A. M., C. F. Raymond, H. Conway, and R. W. Jacobel (2000), Bed properties of Siple Dome and adjacent ice streams, West Antarctica, inferred from radio-echo sounding measurements, *J. Glaciol.*, *46*(152), 88–94, doi:10.3189/172756500781833467.

Jacobel, R. W., B. C. Welch, D. Osterhouse, R. Pettersson, and J. A. MacGregor (2009), Spatial variation of radar-derived basal conditions on Kamb Ice Stream, West Antarctica, *Ann. Glaciol.*, *50*, 10–16, doi:10.3189/172756409789097504.

Joughin, I., J. L. Bamber, T. Scambos, S. Tulaczyk, M. Fahnestock, and D. R. MacAyeal (2006), Integrating satellite observations with modelling: Basal shear stress of the Filcher-Ronne ice streams, Antarctica, *Philos. Trans. R. Soc. A*, *364*, 1795–1814, doi:10.1098/rsta.2006.1799.

Matsuoka, K., D. Morse, and C. F. Raymond (2010), Estimating englacial radar attenuation using depth profiles of the returned power, central West Antarctica, *J. Geophys. Res.*, *115*, F02012, doi:10.1029/2009JF001496.

Matsuoka, K. (2011), Pitfalls in radar diagnosis of ice-sheet bed conditions: lessons from englacial attenuation models, *Geophys. Res. Lett.*, doi:10.1029/2010GL046205, in press.

Muto, A. (2010), Multi-decadal surface temperature trends in East Antarctica inferred from borehole firn temperature measurements and geophysical inverse methods, Ph.D. dissertation thesis, Univ. of Colo. at Boulder, Boulder.

Oswald, G. K. A., and G. D. Q. Robin (1973), Lakes beneath the Antarctic Ice Sheet, *Nature*, *245*, 251–254, doi:10.1038/245251a0.

Pattyn, F. (2010), Antarctic subglacial conditions inferred from a hybrid ice sheet/ice stream model, *Earth Planet. Sci. Lett.*, *295*(3–4), 451–461, doi:10.1016/j.epsl.2010.04.025.

Peters, L. E., S. Anandakrishnan, C. W. Holland, H. J. Horgan, D. D. Blankenship, and D. E. Voigt (2008), Seismic detection of a subglacial lake near the South Pole, Antarctica, *Geophys. Res. Lett.*, *35*, L23501, doi:10.1029/2008GL035704.

Rippin, D. M., J. L. Bamber, M. J. Siegert, D. G. Vaughan, and H. F. J. Corr (2003), Basal topography and ice flow in the Bailey/Slessor region of East Antarctica, *J. Geophys. Res.*, *108*(F1), 6008, doi:10.1029/2003JF000039.

Scambos, T. A., T. M. Haran, M. A. Fahnestock, T. H. Painter, and J. Bohlander (2007), MODIS-based Mosaic of Antarctica (MOA) data sets: Continent-wide surface morphology and snow grain size, *Remote Sens. Environ.*, *111*(2–3), 242–257, doi:10.1016/j.rse.2006.12.020.

Siegert, M. J. (2000), Antarctic subglacial lakes, *Earth Sci. Rev.*, *50*, 29–50, doi:10.1016/S0012-8252(99)00068-9.

Smith, B. E., H. A. Fricker, I. R. Joughin, and S. Tulaczyk (2009), An inventory of active subglacial lakes in Antarctica detected by ICESat (2003–2008), *J. Glaciol.*, *55*(192), 573–595, doi:10.3189/002214309789470879.

Winebrenner, D. P., B. E. Smith, G. A. Catania, H. B. Conway, and C. F. Raymond (2003), Radio-frequency attenuation beneath Siple Dome, West Antarctica, from wide-angle and profiling radar observations, *Ann. Glaciol.*, *37*, 226–232, doi:10.3189/172756403781815483.

M. Albert, Thayer School of Engineering, Dartmouth College, 8000 Cummings Hall, Hanover, NH 03755, USA.

J. Kohler, K. Langley, K. Matsuoka, and J.-G. Winther, Norwegian Polar Institute, Framsenteret, N-9296 Tromsø, Norway. (kirsty@npolar.no)

A. Muto, Department of Geosciences, Pennsylvania State University, 508 Deike Bldg., University Park, PA 16802, USA.

T. Neumann, Cryospheric Science Branch, NASA Goddard Space Flight Center, Code 614.1, Greenbelt, MD 20771, USA.

T. Scambos, National Snow and Ice Data Center, CIRES, University of Colorado at Boulder, 1540 30th St., Boulder, CO 80303, USA.

A. Sinisalo, Department of Geosciences, University of Oslo, PO Box 1047, N-0316 Oslo, Norway.